

Calibrate to Interpret

Gregory Scafarto¹[0000–0002–6544–2358], Nicolas Posocco¹[0000–0002–1795–6039],
and Antoine Bonnefoy¹[0000–0003–1720–7326]

¹ EURA NOVA, Marseille, France

² `firstname.lastname@euranova.eu`

Abstract. Trustworthy machine learning is driving a large number of ML community works in order to improve ML acceptance and adoption. The main aspect of trustworthy machine learning are the followings: fairness, uncertainty, robustness, explainability and formal guaranties. Each of these individual domains gains the ML community interest, visible by the number of related publications. However few works tackle the interconnection between these fields. In this paper we show a first link between uncertainty and explainability, by studying the relation between calibration and interpretation. As the calibration of a given model changes the way it scores samples, and interpretation approaches often rely on these scores, it seems safe to assume that the confidence-calibration of a model interacts with our ability to interpret such model. In this paper, we show, in the context of networks trained on image classification tasks, to what extent interpretations are sensitive to confidence-calibration. It leads us to suggest a simple practice to improve the interpretation outcomes : *Calibrate to Interpret*.

Keywords: Interpretability · Calibration · Classification · Trustworthy Machine Learning ·

1 Introduction

Despite being state of the art on many tasks, deep neural networks (DNNs) are still considered as black boxes which is problematic in contexts where decision making is critical. In order to ensure that a model can be safely used, one needs to have access to the uncertainty over its predictions, and to understand what drives those predictions. Both aspects, namely uncertainty and explainability, are frequently tackled via the use of post-hoc calibration and local interpretation respectively. The current work studies the interaction between these two central aspects of trustworthy machine learning.

There are numerous ways to interpret a model’s behaviour, depending on what one has access to (internal model structure, training phase, ...). This work focuses on methods which interpret the decisions of already trained image classifiers, considering model-aware as well as model-agnostic local interpretation methods, following the definitions given in [33], the former have access to the internal structure of the model while the latter only relies on the predictions scores. These methods provide a saliency map highlighting important pixels for

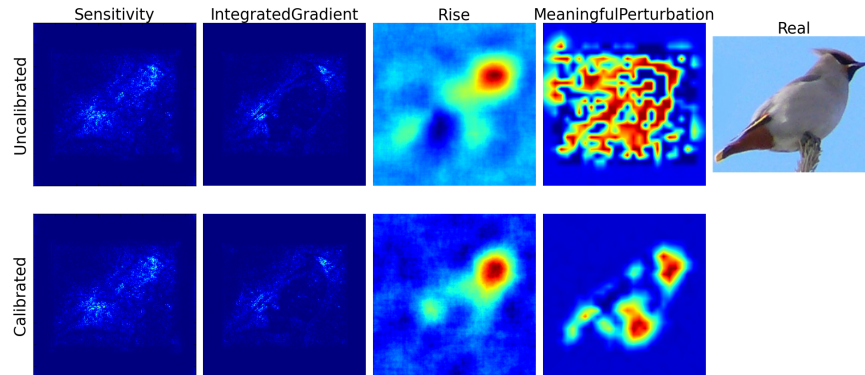


Fig. 1. Visual comparison of saliency changes due to calibration

each prediction. Regarding predictions uncertainty, post-hoc calibration methods adapt models so that their scores are consistent with conditional probabilities related to the predicted class [20]. It is a convenient way to tackle the overconfidence of modern neural networks [11,24].

This focus was made to fit the flexible context in which calibration and interpretation are handled after training the model. Since both post-hoc calibration and local interpretation are linked to the scores associated with the predicted class, we address their interdependence via the following questions: Does calibration impact the saliency maps obtained as interpretations? Do modifications, if any, improve the faithfulness of interpretation methods? Are saliency maps with calibrated models more human-friendly?

Our empirical evaluations highlights that there is indeed a positive interaction between the calibration of a model and its interpretability by enabling some widely used interpretation methods to work more efficiently on it. This impact is visible in terms of faithfulness, visual-coherence of the saliency maps, and their robustness most notably for model-agnostic approaches like Meaningful Perturbation [9]. Examples of saliency maps produced by various methods before and after the calibrations are presented in Figure 1.

After positioning our work in Section 2, we introduce the problems of calibration and local interpretation, as well as the methods used in the literature to tackle them in Section 3. Section 4 then describes the conducted experiments and reports their outcomes. Finally results are discussed and we mention some future works before concluding in Section 5³.

2 Related Works

Trustworthy machine learning has recently gained interest, with the development of modern uncertainty quantification, explainability, robustness, fairness and for-

³ The code is available at : https://github.com/euranova/calibrate_to_interpret

mal guarantees. However few publications have investigated links between these aspects. Among these we can mention attempts to link: robustness and calibration [34,32,43] showing that models which are robust to adversarial attacks are more interpretable; data augmentation, calibration and interpretation showing that MixUp data augmentation greatly impacts the calibration of learnt models [42] and existing saliency methods being used to improve the MixUp procedure itself [15]; or calibration and fairness [29], showing the incompatibility between most of fairness definitions and calibration. Following these works, we study the interaction between two aspects of trustworthy machine learning: uncertainty and explainability via the empirical analysis of the interaction between post-hoc calibration and local interpretation.

3 Problem Statement and other Related Works

Let $x \in \mathbb{R}^{H \times W \times C}$ be an input image and x_i be its features. A model F is trained to classify sample images among C classes. It maps each input x to a logit vector L which is then converted, generally through a softmax function, into an output vector $F(x) \in [0, 1]^C$ so that $\sum_{c=1}^C F(x)_c = 1$. The decision associated with such prediction is $y = \operatorname{argmax}_c F(x)_c$.

3.1 Calibration

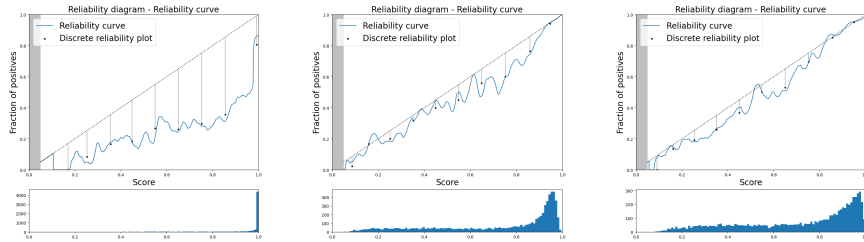


Fig. 2. Confidence reliability plots and curves for VGG16 trained on CIFAR100, when uncalibrated (left, $ECE_{conf} = 0.2$), calibrated using Temperature Scaling (center, $ECE_{conf} = 0.04$) and calibrated with Dirichlet calibration (right, $ECE_{conf} = 0.05$)

Many critical applications motivate the evaluation of confidence-calibration, which indicates how confident a model is in the class it predicts. It is well-known that modern neural networks tend to be miscalibrated, generally overconfident on their predictions [11,24]. Thus some works have been done both on the evaluation of calibration [26] and the improvement of such calibration for a given classifier, would it be during training [21] or as a post-processing step [19,20,28].

As local interpretation allows to interpret each specific predictions, we focused our work on its interaction with confidence-calibration, i.e. the calibration of scores for the predicted class $\operatorname{argmax}(F(x))$.

A model is said to be well confidence-calibrated if:

$$\forall s \in [0, 1], P(y = z \mid F(x)_z = s) = s \quad (1)$$

with $z = \operatorname{argmax}(F(x))$

This notion can be quantified with estimates of the Expected Calibration Error (ECE), defined in the confidence-calibration setting as :

$$ECE^{conf} = ECE^{conf} = \mathbb{E}_{\max(F(X))} [|\mathbb{P}(y = z \mid F(x)_z = s) - s|] \quad (2)$$

In order to calibrate our models, we focus on post-hoc calibration, which can be applied to already trained models and relies exclusively on the scores given by the model. These very nice properties make these approaches plug-and-play, which justifies their popularity. We use in this paper the following techniques, which impact is illustrated in Figure 2.

Temperature scaling If L is the logits vector output of the classifier before softmax activation σ , calibrated scores are given by $F(x)_c^{cal} = \sigma(LT^{-1})_c$ [28]. The temperature scaler T is fit to maximize the likelihood on a holdout set. Its role is to smooth or sharpen predicted scores. It allows DNNs to output more conservative scores, which are generally are over-confident.

Dirichlet calibration Dirichlet calibration [20] considers that score vectors follow a Dirichlet distribution. It transforms $\log(F(x))$ instead of impacting the logits, considering that scores result from a softmax: $F(x)_c^{cal} = \sigma(W \ln(F(x)) + b)_c$, $W \in \mathbb{R}^{c \times c}$ and $b \in \mathbb{R}^c$ being fit on a holdout set.

3.2 Interpretation Methods

We use various methods in our experiments to interpret model’s predictions. They cover a large range of approaches used for interpretation, from model-aware to model-agnostic ones.

Model-aware interpretation While some approaches only use gradient information like the Sensitivity method [37] and Guided Backpropagation [39], others combine such information with a latent representation to understand which input features led to each decision, like Grad-Cam [35] and FullGrad [40]. These gradient-based methods suffer from a few short-comings, such as neurons saturation [36], which have been overcome by methods averaging the gradients over a linear interpolation between the input image and a reference, like Integrated Gradient [41]. Some other methods avoid using gradient and directly use the predicted scores given by the model, to backpropagate it to the input of the model like DeepLIFT [36], a fast algorithm approximating Shapley values. Finally, other methods rank the importance of each latent representation like Score-Cam [45], which relies on a model-aware occlusion based approach.

Model-agnostic interpretation We also use methods that consider interpreted models as black-boxes, such as occlusion-based approaches which degrade the input and analyse predicted score variations to define the importance of each part of the input, like Deletion [5,17], MP [9] or RISE [27]. Others methods use surrogate models in order to locally emulate the complex model behaviour in an interpretable fashion, such as LIME [33] and SHAP [22].

We selected a subset of these interpretation methods. To represent model-agnostic methods, we used RISE and MP, which do not rely on any other information than the output scores of the model for any given input, and Sensitivity, Integrated Gradient for model-aware methods. We also conducted early experiments with other model-aware interpretation methods that were little impacted by calibration, like Grad-CAM, LRP and DeepLIFT, which we chose not to include in this publication to focus on what can be useful to practitioners. Although these approaches are very popular, we did not evaluate LIME and SHAP methods as they are not totally suited for images and are computationally expensive.

Evaluating the validity and limitations of these methods has been the aim of several works [16,2], for example by measuring their sensitivity to adversarial effects [10], their alignment with human perception [23], their faithfulness to the model being explained [13], or their stability [3]. We can rely on these works to build our experimental assessment of the calibration’s impact on interpretations.

4 Evaluation of Calibration’s Impact on Interpretation

4.1 Objectives

Although local interpretation approaches differ, they all rely on the output score vector $F(x)$, which is modified by the calibration process. Our aim is to assess whether or not these modifications have an impact on interpretations, and if this potential impact is rather positive or negative.

Assessing the quality of feature importance - here provided by saliency maps - is challenging, yet we argue that a good interpretation should at least: it should be *faithful* to the model it explains, meaning that removing pixels defined as salient should have an impact on the model outputs [14], interpretations should be *robust* [3], so that similar inputs should lead to similar interpretations, and it should be composed of structured and smoothly-varying components [38], in order to respect human expectations in terms of *visual coherence*.

To evaluate the impact of calibration on interpretations, we first assess if the calibration process actually impacts the resulting saliency maps by making pairwise comparisons between them. We then quantify the impact of these changes by evaluating how the classifier’s confidence drops when progressively removing important features. Third we assess the visual coherence of the produced saliency, by qualifying their structure and smoothly-varying properties, and we finally evaluate the gain in stability of interpretations when calibrating a model.

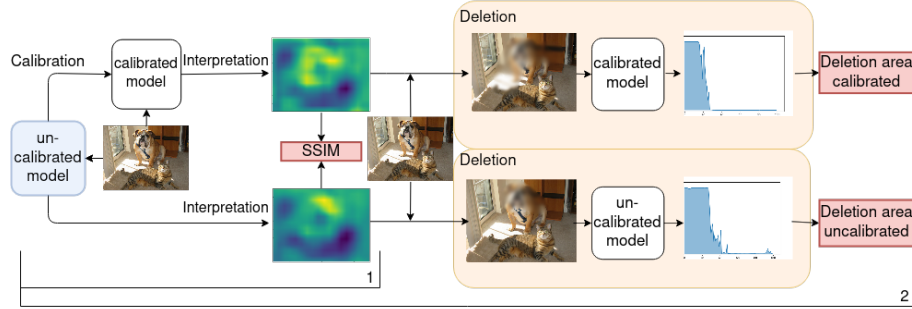


Fig. 3. Protocols to evaluate calibration’s impact on interpretation methods:
 1 - Comparison of interpretations using SSIM, and 2 - Progressive deletion impact

4.2 Experimental Setup

We designed cautiously an experimental setup to ensure the comparison of diverse models, image classification datasets and methods. Our goal was to isolate carefully the impact of the calibration on the interpretation procedures. Post-hoc calibration does not impact the models deeply, hence the observable modifications in interpretations is caused by the calibration step, as we compare the interpretation outcomes on uncalibrated models and their calibrated counterparts, all other things being equal.

Models : The following experiments were conducted with VGG, RESNET and EfficientNet models, classical and diverse architectures for image classification. As DNNs are known to be overconfident [11,24], in practice most pre-trained models available in model zoos are not calibrated, and when applying standard learning algorithm we directly obtain uncalibrated models. Yet, to be able to observe the effect of calibration, the tasks or datasets, should be sufficiently complex for the model, so that the accuracy of the model is not perfect, so that there is no room for calibration improvements.

Datasets : We chose three datasets (of various resolutions) to run our experiments : CIFAR-100[18], Food101[4] and Birds (CUB-200)[44]. These datasets allow a proper use of calibration in its rigorous context, since each image contains exactly one instance of known classes, and they present different visual properties and classification complexities. To ensure reproducible research, we used pretrained models on CIFAR-100 (VGG16 and RESNET50⁴) and Food-101 (ResNet50⁵). As no pre-trained EfficientNet on Birds dataset were available in open access, we fine-tuned (100 epochs with a learning rate of 1e-4 using Adam

⁴ <https://github.com/chenafofo/pytorch-cifar-models>

⁵ <https://github.com/Herick-Asmani/Food-101-classification-using-ResNet-50>

Table 1. Accuracy and confidence-calibration of used models

Model	Dataset	Accuracy	Confidence calibration (ECE^{conf})		
			Base	Temperature	Dirichlet
VGG16	Food101	0.4470	0.1997	0.03	0.063
	Cifar100	0.6811	0.2003	0.0442	0.0477
RESNET32	Cifar100	0.6371	0.1484	0.0463	0.0323
RESNET50	Food101	0.8173	0.0803	0.0323	0.0463
EFFICIENTNETB0	Birds	0.7984	0.0706	0.0234	0.0093

optimizer) an EfficientNet pretrained on ImageNet (from torchvision) onto the Birds dataset.

Calibration : The calibration step has been performed using the calibration methods described previously (Temperature Scaling and Dirichlet calibration). For both methods and every model, we used a calibration set composed of 3000, 2500 and 2500 samples taken from the test set for CIFAR-100, Food-101 and Birds respectively. We evaluated the ECE before and after the calibration using the continuous estimator $ECE_{density}^{conf}$ introduced in [30] using the bandwidth automatically set with Silverman’s rule, on 2500 samples. ECEs and accuracies of the different models, given in Table 1, confirm the initial mis-calibration of the raw models, and the effectiveness of the calibration step.

Interpretation : For Integrated Gradients (IG), black and white references combined are used with 30 equidistant points on the convex path from the reference to the input. For RISE, we randomly sample 4000 8x8 binary masks (higher dimensions would require more sampling), upscale them using bicubic interpolation, and values of the mask are drawn from a 0.6 Bernoulli law. For MP, optimization problems are solved using the Adam optimizer ($\alpha = 0.1, \beta = 0.4, lr = 0.1$) for 600 steps (these optimization parameters have not been fine-tuned).

All computed saliency maps are min-max-normalized. Some of these, resulting from each of the method applied on calibrated and uncalibrated model, can be observed in Figure 1. The saliency maps analyzed in the following experiments were obtained from 2500 images randomly sampled from the remaining test set of each of the datasets (which have not been used for calibration).

4.3 Does Calibration Impact Interpretations ?

We start by comparing each pair of interpretations - coming from uncalibrated and calibrated models - using the structural similarity index (SSIM [46]), which is based on human perception and thus more relevant than MAE or MSE. This experimental protocol is synthesised in Figure 3 part 1.

The results of this experiment, presented in Figure 4, show that for all studied interpretation methods, there is a significant difference between saliency maps

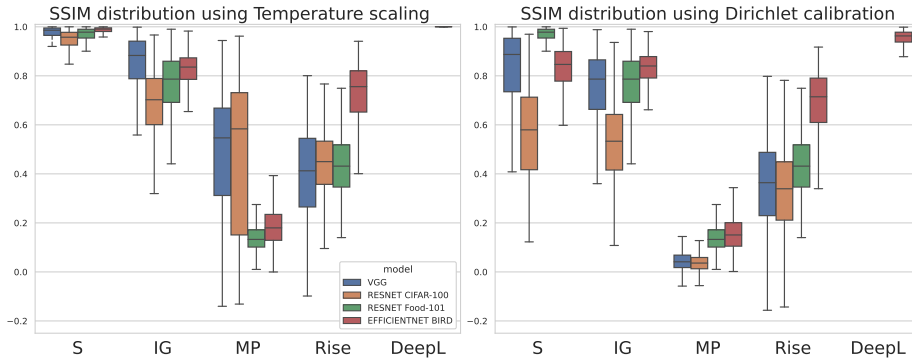


Fig. 4. Distribution of the SSIM between interpretations from calibrated and uncalibrated models

produced from the calibrated and uncalibrated models. This impact is particularly important on model-agnostic interpretation methods like MP and RISE.

4.4 Does Calibration Improve the Faithfulness of Interpretation Methods ?

We further investigate this impact to determine if detected visual changes in saliency maps improve their quality in terms of *faithfulness* [14]. For each pair of interpretations built by the previous experiment, we apply a deletion procedure [27]: input features are ranked according to their importance given by the interpretation, and are progressively neutralized while we observe the impact on the score of the predicted class from the degraded input image. We compute the *deletion area* (area under the score curve wrt to the percentage of neutralized pixels). In practice, to preserve the input’s distribution, neutralized pixels are replaced by an 11x11 gaussian blurred patch ($\sigma = 10$) centered on this pixel. The whole procedure is summed up in Figure 3 part 2.

Additionally to the four interpretation methods we use a random interpretation baseline as reference for the comparison. We remove a given percentage of 100 randomly sorted superpixels computed with the SLIC algorithm [1]. We averaged the deletion curve obtained with five different random orders.

We compute the deletion area on the random baseline, uncalibrated models and calibrated ones. Uncalibrated models are more confident, hence to ensure a fair comparison, we normalize the deletion curves in order to set the score of the predicted class from the initial clean image to one. The normalized curve then shows how much the confidence of the model drops, with respect to its initial confidence, when we neutralize pixels in decreasing importance.

The different interpretation methods show consistent results over the various datasets. Before any calibration considerations, they show very different level of faithfulness, Meaningfull perturbation being the most faithful with a predicted

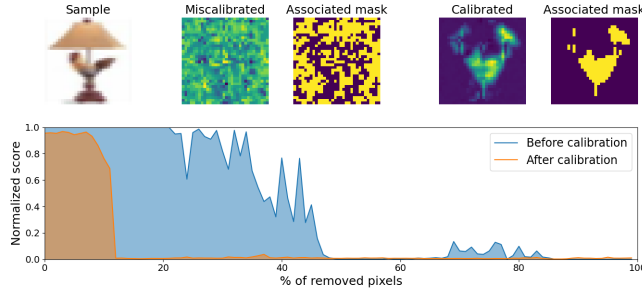


Fig. 5. Saliency maps, Otsu-binarized masks and deletion curves, for the calibrated model and the uncalibrated one, using MP, on a given sample. Map explaining the calibrated model is consistent with human expectation and more faithful to the model.

score quickly dropping as the percentage of neutralized pixels grows, followed by RISE, the other model-agnostic method. MP and RISE are also the most positively impacted by the calibration of the model. These two observations are confirmed by the measurement of the deletion areas shown in the second line of the Figure 7. For the other interpretation methods, the calibration procedure shows little impact, as expected from the SSIM experiment. One can also confirm a posteriori that the normalization of the deletion curves does not introduce any bias, since the same random saliency maps applied to the calibrated and uncalibrated models produce similar curves.

We conduct another analysis to assess the gain that calibration brings in an element-wise comparison of the deletion area. We compare each interpretation with the random baseline and consider that an prediction is well explained if the deletion area is lower for the method than the one obtained with the random saliency. The proportion of well explained images are reported in Figure 7 (third line) as Better Than Random ratio (BTR). This BTR is always improved, except for one model/method case. The improvement varies from limited to important depending on the approach and the dataset. We read the greater impact of the Dirichlet calibration wrt the Temperature scaling, on both the BTR and deletion area, besides that their respective ECE values are cases comparable in most cases, by the fact that Dirichlet calibration can change the predicted class while temperature scaling does not.

The great improvement brought by calibration to MP is promising for model-agnostic interpretation. Notably, it is known that without computationally expensive hyperparameters tuning, MP is sensitive to visual artifacts [8]. As the example in Figure 5 suggests, calibration seems to help dealing with those.

To sum up, we measure a positive impact on the faithfulness as measured by the deletion area and the BTR ratio presented in Section 4.4 for model-agnostic methods, in worst case the interpretability is not impacted by the calibration. The most faithful method without calibration, namely MP, is also the most

improved method. This suggests that the interpretability of the model in itself could depend on its calibration.

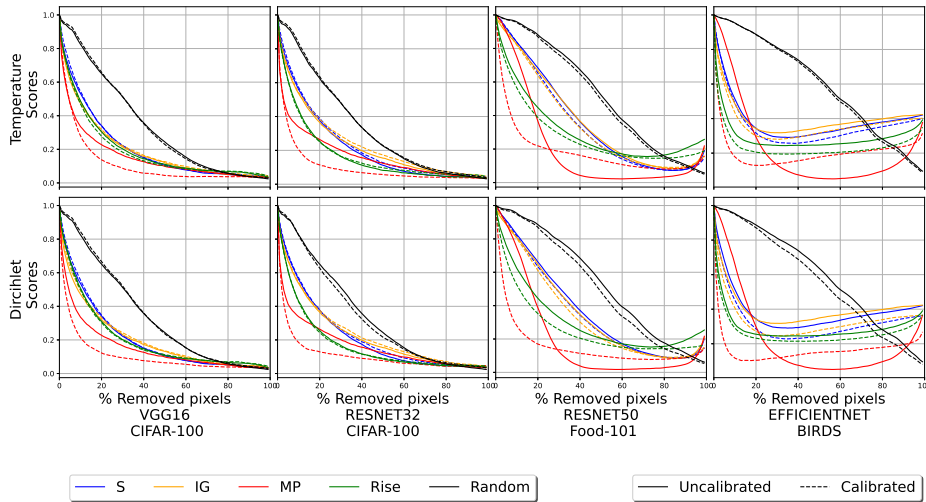


Fig. 6. Deletion curves before (plain line) and after calibration (dashed line) for three different models using Temperature Scaling (upper) and Dirichlet calibration (lower)

4.5 Are Saliency Maps with Calibration more Human-Friendly ?

Another important aspect of interpretation is the readability for users, smoothly varying saliency maps are easier to comprehend, as they tend to highlight structures that we, as humans, recognize. Therefore, to quantify the complexity of a produced saliency map, we first distinguish activated pixels (foreground of saliency maps) from non-activated ones (background) using Otsu binarization [25], and compute the total variation (TV) of obtained binary images. A higher total variation suggests a more noisy interpretation.

Figure 7 shows that Otsu-TV is always improved (lowered) by calibration for model-agnostic methods, or at worst unaffected for other methods, which means that interpretations exhibit smoother variations and fewer highlighted regions, while the mean deletion area is constant or improved. Hence the interpretations of the calibrated models are more human readable while being equally or more faithful to the model.

4.6 In Depth Analysis of Meaningful Perturbation

To better understand our findings, we focus now on MP, the most faithful method, which appears to be the most impacted by the calibration.



Fig. 7. Ratio of well explained images (BTR Ratio), Otsu-binarized TV and Deletion Area obtained by various interpretation methods on multiple models and datasets before and after calibration.

Effect of the mis-calibration In order to evaluate if, for MP, the faithfulness improvement correlates with the mis-calibration level, we apply the deletion experiment using Temperature Scaling for different fixed temperatures. Figure 8 highlights that the minimum of the deletion area is obtained when the model is calibrated, showing a clear non linear correlation between the scaler’s temperature value and the deletion area. Interestingly the second plot highlights a positive correlation between the mean AUC (deletion area) and the ECE. The correlation differs whether the mis-calibration is due to an overconfident model or an underconfident model for the same range of ECE. The overconfident models are those with a temperature smaller than the best obtained.

Interpretation stability As shown previously, calibration improves the deletion area and the total variation of saliency maps from MP, the best method in terms of deletion area, meaning that produced interpretations are both more faithful (according to [14] definition) and more spatially coherent. One possible explanation for this improvement is that calibration improves the stability of the method. It is known that MP is sensitive to visual artifacts [8] without proper hyperparameters tuning. Calibration seems to be a really adequate solution to prevent the apparition of such artifacts, especially when parameter tuning is not feasible. Indeed, as underlined in [3], interpretation methods tend to be unstable when the input is slightly modified. As calibration is related to the model’s robustness [32] it is natural to wonder whether or not the calibration of a given model improves the robustness of the interpretations made on its predictions. To that end, we compute an approximation of the Lipschitz

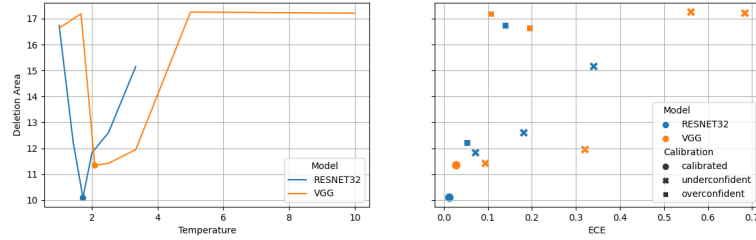


Fig. 8. Mean deletion area on CIFAR-100 for VGG16 and RESNET32 conditioned on the temperature. Marked points indicate calibrated models.

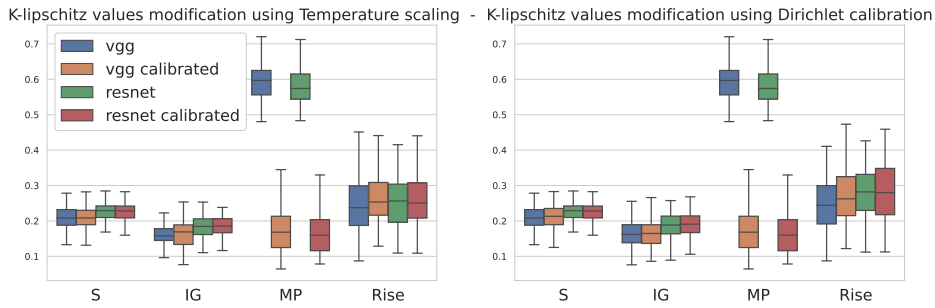


Fig. 9. K-lipschitz distribution obtained with calibrated and uncalibrated model using Temperature Scaling (left) and Dirichlet calibration (right).

constant of the saliency function, following the experiment introduced in [3], by adding small amount of gaussian noise to the input, so that the behaviour of the model does not change, and compute the normalized l_2 -norm of the interpretations obtained with and without calibration. This experiment was applied on 150 randomly sampled points from CIFAR-100. For each point, we sample 40 neighbour points (inside the ball of radius 0.05 and with the point of interest as center). We only apply this experiments on 150 points in order to keep it feasible in a reasonable amount of time (for MP and Rise processing each point takes around an hour with an NVIDIA 1650).

Figure 9 reveals that calibration, while having no robustness impact on most methods, considerably improves the stability of MP. This is consistent with the $10\times$ decrease of TV for MP revealed in the previous section. Also, RISE, which is the least stable even after calibration, could be improved by increasing the number of sampled masks at the expense to an higher computational cost.

4.7 Discussions

While these results shed light on non-trivial interaction between interpretation methods and calibration, it is hard to express from the gain in term of deletion area a definitive statement about interpretation methods validity. This come

from the difficulty of evaluating explanation and therefore to the best of our knowledge no consensus has been attained in terms of the best method to validate interpretation methods. The deletion experiments, while truly evaluating interpretations quality, seems to favor methods which highlight regions over methods which highlight high frequency details, which would account for the poor faithfulness performance as measured by the deletion area. Moreover, we are convinced that a good interpretation method should be able to reflect the uncertainty of the model and therefore should be impacted by the calibration, we even argue that this could be a clue to setup a new sanity check for interpretation methods.

5 Conclusions and Future works

This paper studies the relationship between uncertainty and explainability, two important aspects of trustworthy machine learning. More specifically we evaluate the impact of post-hoc calibration of a given image classification model over the quality of the saliency maps produced by several widely used local interpretation methods applied on the model for different datasets and models. The experimental benchmark, built to evaluate this impact *all other things being equal*, shows a positive impact of calibration on produced interpretations, in terms of faithfulness, stability and visual coherence. The impact, particularly beneficial on model-agnostic interpretation methods such as Meaning Perturbation (MP) [9], is in the worst case neutral. For these reasons, we suggest a simple practice to improve interpretation outcomes : *Calibrate to Interpret*.

A side benefit of the study is to rank the competing interpretation approaches, which shows that model-agnostic ones perform better with regard to faithfulness, measured by the deletion area, and visual coherence, measured by the Otsu-TV. Interestingly the stronger impact of calibration appears on the best interpretation method namely MP, and resolves one of its main drawbacks: its sensitivity to artifacts. We highlight for this method that there is a clear correlation between the calibration level of a model and the faithfulness of the MP method applied to its predictions.

This work opens the road to deeper analyses. A direct extension would be to analyse if *in-training* solutions to enforce calibration would impact similarly the interpretations. This would require a different benchmark setup, where modifications induced to the model by *in-training* calibration are properly framed. Additionally, although computational cost considerations prevented us from realizing experiments with the ROAR procedure [12] to measure the faithfulness of interpretation methods, we think the theoretical properties of this approach make it a great option to deepen our experimental evaluation. Finally, we wonder if other kinds of explanation paradigm, e.g. concept based [6], sample based [31] or even attention based [7] can also benefit from calibration.

References

1. Achanta, R., Shaji, A., Smith, K., Lucchi, A., Fua, P., Süsstrunk, S.: Slic superpixels compared to state-of-the-art superpixel methods. *IEEE Transactions on Pattern Analysis and Machine Intelligence* **34**(11), 2274–2282 (2012). <https://doi.org/10.1109/TPAMI.2012.120>
2. Adebayo, J., Gilmer, J., Muelly, M., Goodfellow, I., Hardt, M., Kim, B.: Sanity checks for saliency maps. In: *Advances in Neural Information Processing Systems*. p. 9525–9536. NIPS’18, Curran Associates Inc., Red Hook, NY, USA (2018)
3. Alvarez-Melis, D., Jaakkola, T.S.: On the robustness of interpretability methods. arXiv preprint arXiv:1806.08049 (2018)
4. Bossard, L., Guillaumin, M., Van Gool, L.: Food-101 – mining discriminative components with random forests. In: *European Conference on Computer Vision* (2014)
5. Chang, C.H., Creager, E., Goldenberg, A., Duvenaud, D.: Explaining image classifiers by counterfactual generation. In: *International Conference on Learning Representations* (2019)
6. Chen, C., Li, O., Tao, C., Barnett, A.J., Su, J., Rudin, C.: This looks like that: deep learning for interpretable image recognition. In: *Advances in Neural Information Processing Systems*. p. 8928–8939 (2019)
7. Chen, M., Radford, A., Child, R., Wu, J., Jun, H., Luan, D., Sutskever, I.: Generative pretraining from pixels. In: *International Conference on Machine Learning*. pp. 1691–1703. PMLR (2020)
8. Fong, R., Vedaldi, A.: Interpretable explanations of black boxes by meaningful perturbation. pp. 3449–3457 (10 2017). <https://doi.org/10.1109/ICCV.2017.371>
9. Fong, R.C., Vedaldi, A.: Interpretable explanations of black boxes by meaningful perturbation. In: *2017 IEEE International Conference on Computer Vision (ICCV)*. pp. 3449–3457 (2017). <https://doi.org/10.1109/ICCV.2017.371>
10. Ghorbani, A., Abid, A., Zou, J.: Interpretation of neural networks is fragile. *Proceedings of the AAAI Conference on Artificial Intelligence* **33**(01), 3681–3688 (Jul 2019). <https://doi.org/10.1609/aaai.v33i01.33013681>, <https://ojs.aaai.org/index.php/AAAI/article/view/4252>
11. Guo, C., Pleiss, G., Sun, Y., Weinberger, K.Q.: On calibration of modern neural networks. In: Precup, D., Teh, Y.W. (eds.) *Proceedings of the 34th International Conference on Machine Learning*. *Proceedings of Machine Learning Research*, vol. 70, pp. 1321–1330. PMLR (06–11 Aug 2017), <http://proceedings.mlr.press/v70/guo17a.html>
12. Hooker, S., Erhan, D., Kindermans, P.J., Kim, B.: Evaluating feature importance estimates (2018)
13. Hooker, S., Erhan, D., Kindermans, P.J., Kim, B.: A benchmark for interpretability methods in deep neural networks. In: Wallach, H., Larochelle, H., Beygelzimer, A., d'Alché-Buc, F., Fox, E., Garnett, R. (eds.) *Advances in Neural Information Processing Systems* 32, pp. 9737–9748. Curran Associates, Inc. (2019), <http://papers.nips.cc/paper/9167-a-benchmark-for-interpretability-methods-in-deep-neural-networks.pdf>
14. Jacovi, A., Goldberg, Y.: Towards faithfully interpretable nlp systems: How should we define and evaluate faithfulness? arXiv preprint arXiv:2004.03685 (2020)
15. Kim, J.H., Choo, W., Song, H.O.: Puzzle mix: Exploiting saliency and local statistics for optimal mixup. In: *International Conference on Machine Learning*. pp. 5275–5285. PMLR (2020)

16. Kindermans, P.J., Hooker, S., Adebayo, J., Alber, M., Schütt, K.T., Dähne, S., Erhan, D., Kim, B.: The (Un)reliability of Saliency Methods, pp. 267–280. Springer International Publishing, Cham (2019). https://doi.org/10.1007/978-3-030-28954-6_14, https://doi.org/10.1007/978-3-030-28954-6_14
17. Kononenko, I., Robnik-Sikonja, M.: Explaining classifications for individual instances. *IEEE Transactions on Knowledge & Data Engineering* **20**(05), 589–600 (may 2008). <https://doi.org/10.1109/TKDE.2007.190734>
18. Krizhevsky, A., Hinton, G., et al.: Learning multiple layers of features from tiny images (2009)
19. Kull, M., Filho, T.S., Flach, P.: Beta calibration: a well-founded and easily implemented improvement on logistic calibration for binary classifiers. In: Singh, A., Zhu, J. (eds.) *Proceedings of the 20th International Conference on Artificial Intelligence and Statistics. Proceedings of Machine Learning Research*, vol. 54, pp. 623–631. PMLR (20–22 Apr 2017), <https://proceedings.mlr.press/v54/kull117a.html>
20. Kull, M., Nieto, M.P., Kängsepp, M., Silva Filho, T., Song, H., Flach, P.: Beyond temperature scaling: Obtaining well-calibrated multi-class probabilities with dirichlet calibration. In: *Advances in Neural Information Processing Systems*. pp. 12295–12305 (2019)
21. Kumar, A., Sarawagi, S., Jain, U.: Trainable calibration measures for neural networks from kernel mean embeddings. In: Dy, J., Krause, A. (eds.) *Proceedings of the 35th International Conference on Machine Learning. Proceedings of Machine Learning Research*, vol. 80, pp. 2805–2814. PMLR (10–15 Jul 2018), <http://proceedings.mlr.press/v80/kumar18a.html>
22. Lundberg, S.M., Lee, S.I.: A unified approach to interpreting model predictions. In: Guyon, I., Luxburg, U.V., Bengio, S., Wallach, H., Fergus, R., Vishwanathan, S., Garnett, R. (eds.) *Advances in Neural Information Processing Systems*. vol. 30. Curran Associates, Inc. (2017)
23. Mohseni, S., Block, J.E., Ragan, E.: Quantitative evaluation of machine learning explanations: A human-grounded benchmark. In: *26th International Conference on Intelligent User Interfaces*. p. 22–31. IUI '21, Association for Computing Machinery, New York, NY, USA (2021). <https://doi.org/10.1145/3397481.3450689>, <https://doi.org/10.1145/3397481.3450689>
24. Nguyen, A., Yosinski, J., Clune, J.: Deep neural networks are easily fooled: High confidence predictions for unrecognizable images. In: *2015 IEEE Conference on Computer Vision and Pattern Recognition (CVPR)*. pp. 427–436 (2015). <https://doi.org/10.1109/CVPR.2015.7298640>
25. Otsu, N.: A threshold selection method from gray-level histograms. *IEEE Transactions on Systems, Man, and Cybernetics* **9**(1), 62–66 (1979). <https://doi.org/10.1109/TSMC.1979.4310076>
26. Pakdaman Naeini, M., Cooper, G., Hauskrecht, M.: Obtaining well calibrated probabilities using bayesian binning. *Proceedings of the AAAI Conference on Artificial Intelligence* **29**(1) (Feb 2015), <https://ojs.aaai.org/index.php/AAAI/article/view/9602>
27. Petsiuk, V., Das, A., Saenko, K.: Rise: Randomized input sampling for explanation of black-box models. In: *BMVC* (2018)
28. Platt, J.C.: Probabilistic outputs for support vector machines and comparisons to regularized likelihood methods. In: *ADVANCES IN LARGE MARGIN CLASSIFIERS*. pp. 61–74. MIT Press (1999)
29. Pleiss, G., Raghavan, M., Wu, F., Kleinberg, J., Weinberger, K.Q.: On fairness and calibration. *Advances in neural information processing systems* **30** (2017)

30. Posocco, N., Bonnefoy, A.: Estimating expected calibration errors. In: Farkaš, I., Masulli, P., Otte, S., Wermter, S. (eds.) *Artificial Neural Networks and Machine Learning – ICANN 2021*. pp. 139–150. Springer International Publishing, Cham (2021)
31. Pruthi, G., Liu, F., Kale, S., Sundararajan, M.: Estimating training data influence by tracing gradient descent. In: Larochelle, H., Ranzato, M., Hadsell, R., Balcan, M.F., Lin, H. (eds.) *Advances in Neural Information Processing Systems*. vol. 33, pp. 19920–19930. Curran Associates, Inc. (2020), <https://proceedings.neurips.cc/paper/2020/file/e6385d39ec9394f2f3a354d9d2b88eec-Paper.pdf>
32. Qin, Y., Wang, X., Beutel, A., Chi, E.: Improving uncertainty estimates through the relationship with adversarial robustness (06 2020)
33. Ribeiro, M.T., Singh, S., Guestrin, C.: "why should i trust you?": Explaining the predictions of any classifier. In: *Proceedings of the 22nd ACM SIGKDD International Conference on Knowledge Discovery and Data Mining*. p. 1135–1144. KDD '16, Association for Computing Machinery (2016). <https://doi.org/10.1145/2939672.2939778>
34. Ross, A.S., Doshi-Velez, F.: Improving the adversarial robustness and interpretability of deep neural networks by regularizing their input gradients. In: *AAAI conference on artificial intelligence* (2018)
35. Selvaraju, R.R., Cogswell, M., Das, A., Vedantam, R., Parikh, D., Batra, D.: Grad-cam: Visual explanations from deep networks via gradient-based localization. In: *2017 IEEE International Conference on Computer Vision (ICCV)*. pp. 618–626 (2017). <https://doi.org/10.1109/ICCV.2017.74>
36. Shrikumar, A., Greenside, P., Kundaje, A.: Learning important features through propagating activation differences. In: Precup, D., Teh, Y.W. (eds.) *Proceedings of the 34th International Conference on Machine Learning*. *Proceedings of Machine Learning Research*, vol. 70, pp. 3145–3153. PMLR (06–11 Aug 2017), <http://proceedings.mlr.press/v70/shrikumar17a.html>
37. Simonyan, K., Vedaldi, A., Zisserman, A.: Deep inside convolutional networks: Visualising image classification models and saliency maps. *CoRR* **abs/1312.6034** (2014)
38. Smilkov, D., Thorat, N., Kim, B., Viégas, F., Wattenberg, M.: Smoothgrad: removing noise by adding noise. *arXiv preprint arXiv:1706.03825* (2017)
39. Springenberg, J.T., Dosovitskiy, A., Brox, T., Riedmiller, M.A.: Striving for simplicity: The all convolutional net. *CoRR* **abs/1412.6806** (2015)
40. Srinivas, S., Fleuret, F.: Full-gradient representation for neural network visualization. In: *Advances in Neural Information Processing Systems* (2019)
41. Sundararajan, M., Taly, A., Yan, Q.: Axiomatic attribution for deep networks. *JMLR.org* (2017)
42. Thulasidasan, S., Chennupati, G., Bilmes, J., Bhattacharya, T., Michalak, S.: On mixup training: Improved calibration and predictive uncertainty for deep neural networks. *arXiv preprint arXiv:1905.11001* (2019)
43. Tsipras, D., Santurkar, S., Engstrom, L., Turner, A., Madry, A.: Robustness may be at odds with accuracy (2018), <http://arxiv.org/abs/1805.12152>, cite arXiv:1805.12152
44. Wah, C., Branson, S., Welinder, P., Perona, P., Belongie, S.: *The Caltech-UCSD Birds-200-2011 Dataset*. Tech. Rep. CNS-TR-2011-001, California Institute of Technology (2011)
45. Wang, H., Wang, Z., Du, M., Yang, F., Zhang, Z., Ding, S., Mardziel, P., Hu, X.: Score-cam: Score-weighted visual explanations for convolutional neural net-

- works. In: 2020 IEEE/CVF Conference on Computer Vision and Pattern Recognition Workshops (CVPRW). pp. 111–119 (2020). <https://doi.org/10.1109/CVPRW50498.2020.00020>
46. Wang, Z., Bovik, A.C., Sheikh, H.R., Simoncelli, E.P.: Image quality assessment: From error visibility to structural similarity. *IEEE Transactions on Image Processing* **13**(4), 600–612 (2004)

Supplementary Material

A Interpretation method details

Model aware interpretation methods The *Sensitivity* saliency map shows the sensitivity of the output to infinitesimal changes in each input feature. It is obtained by simply taking the derivative of the score w.r.t to the input :

$$S_{x,F}(x_i) = \sum_{channels} \frac{\partial F(x)_c}{\partial x}(x_i) \quad (3)$$

Integrated Gradient improves on the Sensitivity method and avoids the null gradient issue by computing the average of gradients obtained for images along the convex path created by the interpolation between the input image and a reference image. Given x^r the reference image, the formula used practically is :

$$S_{x,F}(x_i) = \frac{(x_i - x_i^r)}{m} \sum_{k=1}^m \frac{\partial F(x_i^r + \frac{k}{m}(x_i - x_i^r))}{\partial x}(x_i) \quad (4)$$

Finally, *LayerWise Relevance Propagation* (LRP) was used. It belongs to the family of interpretation algorithms that leverage the inside architecture of the model but without relying on the gradients. It backpropagates the output score $F(x)_c$ through the model through a signal called relevance. The main rule is the conservation of the relevance between layers, the sum of all relevances of a layer should be equal to the output score :

$$\forall l, F(x)_c \approx \sum_p R_p^{(l)} \quad (5)$$

To do so the score is backpropagated from one neuron to another proportionally to each neuron activation and to the strength of the link between them.

$$R_j^l = \sum_k \frac{a_j w_{jk}}{\epsilon + \sum_{0,j} a_j w_{jk}} R_k^{l+1} \quad (6)$$

with $w_{j,k}$ the weight between the neuron j of the l -th layer and k , a_j the activation of the j -th neuron of the $l+1$ -th layer and ϵ a jitter parameter which stabilizes numerically the propagation.

Model agnostic interpretation methods We also used methods that consider models as black-boxes such as occlusion-based approaches which degrade the input and analyse predicted score variations to define the importance of each part of the input. We used RISE and Meaningful Perturbation in our experiments.

RISE's saliency map is obtained by computing the sum of randomly sampled masks weighted by the scores obtained when the model is applied to these masked

image. Given a certain mask m_j and the number of samples N , we have :

$$S_{x,F}(x_i) = \frac{1}{\mathbb{E}([m]) * N} \sum_{j=1}^N F(I \odot m_j)(x_i) \quad (7)$$

Meaningful Perturbation (MP) tries to find the smallest mask which makes the prediction score drop the most by optimizing :

$$\min_{m \in [0,1]^{H*W}} \lambda \|1 - m\|_1 + \beta TV(m) + F(x \odot m)_c \quad (8)$$

with TV being the total variation of the mask. This parameter penalizes the shape of the mask to be as regular as possible in order to avoid adversarial artifacts.